(Received 24 February 2024, Accepted 15 July 2024, Scheduled 8 August 2024)

Design of CPW-Fed Flexible Fractal Shape Circular Ring Patch Antenna for Biomedical Applications at ISM Band

Pasumarthi Amala Vijaya Sri[1] and Ketavath Kumar Naik[2,*]

[1]*Department of Electronics and Communication Engineering*
Vignan's Lara Institute of Technology & Science, Vadlamudi, Guntur, AP, India
[2]*Antenna Research Lab, Department of Electronics and Communication Engineering*
Koneru Lakshmaiah Education Foundation (KLEF) deemed to be University
Vaddeswaram, Guntur, AP, India

ABSTRACT: A CPW-fed flexible fractal shape circular ring patch (FSCRP) antenna is presented in this paper and operates at ISM band for biomedical applications. The proposed antenna operates at 2.46 GHz both in free space and on a human hand. This antenna functions within a 10 dB impedance bandwidth of 390 MHz (2.38 GHz to 2.77 GHz) in free space and 800 MHz (2.04 GHz to 2.84 GHz) on human hand structure with a reflection coefficient of −33.9 dB and −36.97 dB, respectively. The circular shape fractal structure operates the antenna with circular polarization, and a 3 dB axial ratio of 170 MHz (2.4 GHz to 2.57 GHz) has been observed. The proposed antenna can be used in Implantable Medical Devices (IMDs) for biotelemetry applications. The simulated and measured results for the proposed FSCRP antenna are also presented in this paper.

1. INTRODUCTION

With the increase in the demand of implantable medical devices (IMDs) for patient monitoring, flexible patch antennas with compactness and biocompatibility are preferable. Antennas are used as a communication interface between the external device and IMDs. The major factors to be considered while designing implantable antennas are patient safety, power consumption, compact size, polarization issues, sufficient radiation efficiency, and many others [1–3]. From the literature survey, the antenna miniaturization was considered by tracking the high dielectric constant of the substrate [4] and radiating patch with slots [5], which reduces the ineffective size of the antenna. Similarly, a compact patch antenna [6], with inset feed and c-slot has been designed for on-body communication. Koch fractal dipole antenna [7] and antenna with aircraft shape badge [8] have been designed for on-body wearable military applications. A flexible implantable loop antenna [9] was designed for biomedical telemetry application. In this study, a complementary split ring resonator is considered to operate for medical device radio communication services (MedRad — 401–406 MHz) and ISM band. The antenna models were designed with linear polarization, where multi-fading distortion is observed. The multi-fading effect can be eliminated by designing the antenna with circular polarization.

In [10], a planar inverted-F antenna with two skin-implantable biotelemetry devices has been considered to operate antenna for Medical Implant Communication System (MICS) and ISM band. The electrical properties of human tissues are considered [11], to operate antenna at medical band frequency. A conformal patch antenna with slots and splits [12] has been designed for an antenna to operate for ISM band biomedical applications and for a frequency range of 2.41 to 2.81 GHz with a bandwidth of 400 MHz, and minimum gain of −19.6 dB at 2.6 GHz has been obtained. An artificial magnetic structure was introduced in [13] to reduce the interference between the antenna and the human body. This antenna resonates at 2.45 GHz frequency and is used for wireless body area networks (WBAN). Swastika shape slot [14] and asymmetric T-shape antenna in [15] have been designed for on-body WBAN applications. Along with biocompatibility, temperature sensors can help maintain comfortable conditions for patients by reducing stress and promoting faster recovery which Is also a major issue to ensure the safety of the patient [16, 17]. The posting of the proposed antenna in implantable devices and the distance between the transmitters for gathering the patient information is the major issue to be considered. So the antenna should be placed in implantable device in an adequate area and by maintaining an appropriate angle during surgery. However, robust communication needs to be done between the patient and the exterior device. Therefore, it is desired to employ an antenna that is independent of the orientation of the transmitter and receiver.

A pentagon-shaped antenna with a Y-shaped electromagnetic coupled feed line was designed [18] for both indoor and outdoor wearable applications. A triangular dielectric resonator antenna [19] with facet spiral fed and square shape patch antenna with three shorting pins has been considered [20], for biomedical application. In [20], an antenna operates for 2.4 GHz ISM band with an impedance bandwidth of 6.2% has been observed.

* Corresponding author: Ketavath Kumar Naik (drkumarkn@hotmail.com).

A rectangle-shaped patch antenna with a ground plane greater than the patch was designed in [21], to operate from 902 MHz to 928 MHz frequency band with a bandwidth of 18.2% for ISM band application. In [22], an antenna design with metallic pins and meander slots has been considered to an antenna operating for 915 MHz ISM band frequency with bandwidths of 889 to 924 MHz respectively. In [23], a circularly polarized antenna with square truncated corners and cross slots has been designed for ISM band application with operating frequency of 915 MHz, impedance bandwidth of 10.6% (865–962 MHz), and axial ratio bandwidth of 14 MHz, respectively. Similarly, in [24], an antenna was designed for the 2.45 GHz ISM band. A compact size of $10 \times 10 \times 0.4\,\text{mm}^3$ has been considered in [25], and an annular ring shape patch antenna with shorting pins and an L-shaped open-end slot was designed for ISM band application. In [26], an impedance bandwidth of 8% (2.4 to 2.48 GHz) has been observed. A spherical shape antenna [27], a split ring resonator shape antenna in [28], a circular shape antenna with open-ended slots in [29], a patch antenna with parasitic element [30], and a planar inverted F-shape antenna (PIFA) [31] were designed for biomedical application. In [27], the radiation efficiency of 3.3% and in [28] an ultra-wide bandwidth of 138.7% have been observed. In [31], an antenna with planar and conformal structures has been designed to operate at Internet of Medical Things (IoMT) for biotelemetry applications with a bandwidth of 134 MHz and 142 MHz, respectively. However, insufficient literature is observed to the design of ISM band antenna with fractal structures and coplanar waveguide (CPW) feed with circular polarization.

In this paper, a novel design of flexible fractal shape circular ring patch (FSCRP) antenna with CPW-fed is presented for ISM band and circular polarization. The analysis of the FSCRP antenna model is carried out in free space and a multi-layer human tissue environment. The antenna resonates at 2.46 GHz frequency, and an impedance bandwidth of 390 MHz in free space and 800 MHz on multi-layer tissue model is observed. The work is arranged as follows. Section 1 provides an introduction, and Section 2 explains the proposed antenna design and analysis. The evaluation process is explained in Section 3. The results are discussed and presented in Section 4.

2. ANTENNA GEOMETRY

The proposed antenna is designed with a flexible fractal shape circular ring patch (FSCRP) fed through a CPW feed line. The FSCRP antenna is fabricated on a polyimide substrate material with ε_r 3.5, length (L_1), width (W_1), and height (h) 0.07 mm as shown in Fig. 1. The circular ring shape patch with outer diameter d_1 and ring width S_1 is coated with copper material on the substrate material. The fractal structure is obtained by considering circular ring and triangular shape patches as given in Fig. 1. The dimensions of the circular ring outer diameter and ring width are d_2, s_2, and the dimensions of the triangular shape fractal structure are h_1, h_2, respectively.

The FSCRP antenna model is fed through a CPW having an input feed of 50 Ω. The feeding strip line has a length of L_2 and a width of W_2 through a rectangular patch. The length and width of the CPW feed along the x and y axis are L_3 and W_3 respectively. The optimized FSRCP antenna parameters are tabulated in Table 1.

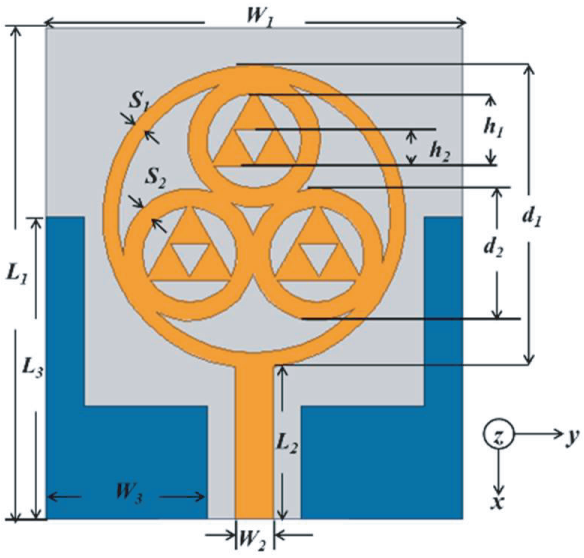

FIGURE 1. The FSCRP antenna model.

TABLE 1. Geometric value of FSCRP antenna model.

Parameter	Value (mm)	Parameter	Value (mm)
L_1	26	d_1	16
W_1	22	d_2	7
L_2	8	h_1	4
W_2	2	h_2	1.8
L_3	16	S_1	0.8
W_3	8.5	H	0.07

The FSCRP antenna operates at the 2.46 GHz ISM band. The two shorting structures and a folded ground plane are considered for a compact size and low profile of the proposed model. The circular polarization is generated due to the circle-shaped ring patches added to the circular ring antenna. The FSCRP antenna model analysis is performed by placing the antenna in free space, on the multi-layer tissue structure (skin, fat, muscle) of the human body as presented in Fig. 2. The height of the skin tissue is 2 mm, and those of fat and muscle tissues are 4 mm. The dielectric property of the human tissues [18] at 2.45 GHz frequency is depicted in Table 2.

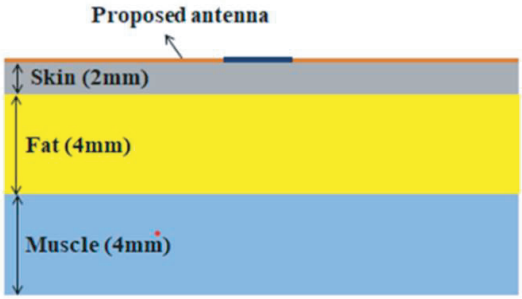

FIGURE 2. Layered model of the human tissue.

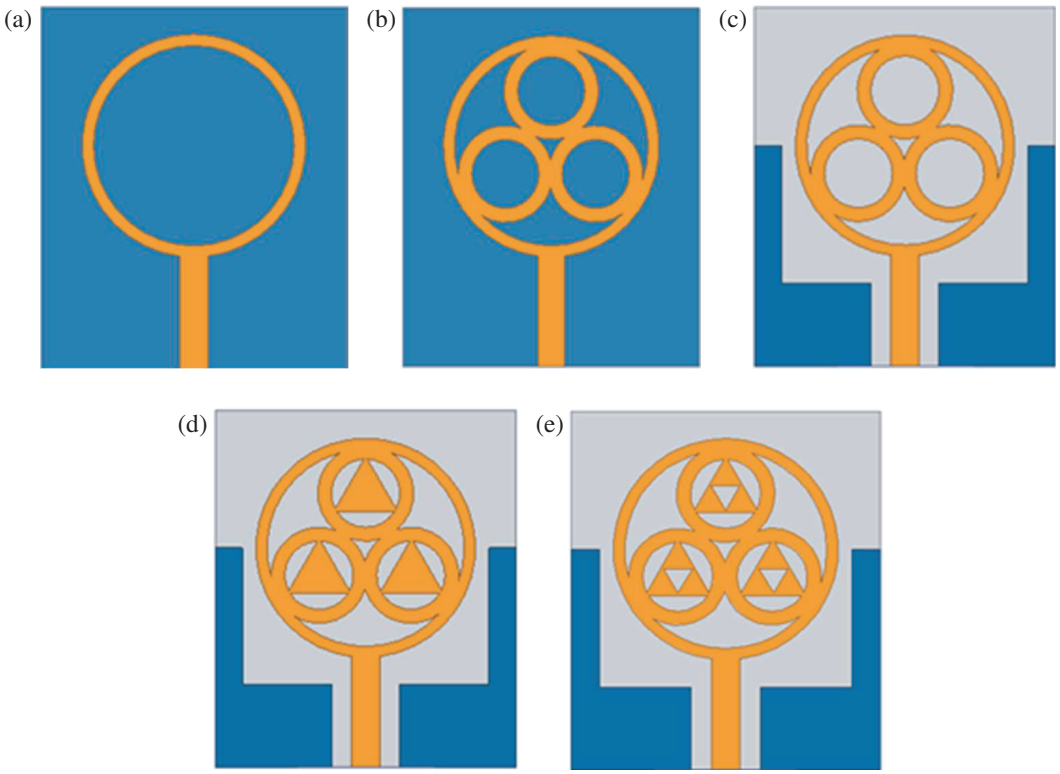

FIGURE 3. Evaluation process of the FSCRP antenna model, (a) to (e).

TABLE 2. Human tissues properties at 2.45 GHz frequency.

Biological Tissue	Permittivity (ε_r)	Conductivity (S/m)	Height (mm)
Skin	37.45	1.74	2
Fat	5.22	0.13	4
Muscle	52.06	2.14	4

3. EVALUATION PROCESS OF PROPOSED ANTENNA

The evaluation for the proposed FSCRP antenna model is performed step-by-step as presented in Fig. 3. In the first step, a circular ring shape patch antenna (Ant-1) is considered with a full ground plane, shown in Fig. 3(a). This antenna operates at 2.48 GHz frequency with a minimum reflection coefficient (S_{11}) of -8.7 dB. In the second step, three circular ring patches are integrated into the outer circular ring (Ant-2) as shown in Fig. 3(b), and it resonates at 2.7 GHz with -5.7 dB reflection coefficient. The CPW feed is considered to be Ant-2 and presented in Fig. 3(c). This antenna (Ant-3) resonates at 2.58 GHz with a reflection coefficient of -15.78 dB and a bandwidth of 2.41–2.8 GHz.

Figure 3 presents the evaluation process of the FSCRP antenna model, (a) to (e). To improve S_{11} and operating frequency, the triangular shape patches are integrated into the three circular ring patches (Ant-4) as presented in Fig. 3(d). Ant-4 resonates at 2.48 GHz frequency with a reflection coefficient -20.7 dB and a bandwidth of 2.4–2.78 GHz. In the final iteration, Ant-5 is designed by adding a triangular shape slot as shown in Fig. 3(e). The FSCRP antenna model operates at 2.46 GHz frequency with a reflection coefficient -33.7 dB and impedance bandwidth of 380 MHz, respectively. The S_{11} plot for the five antenna models is presented in Fig. 4.

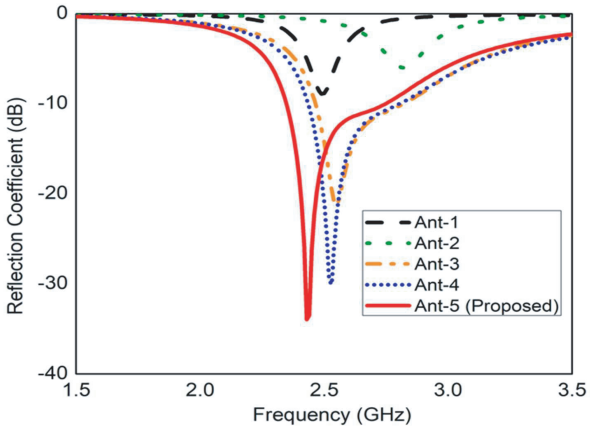

FIGURE 4. Reflection Coefficient plot for evaluation process.

4. RESULTS AND DISCUSSION

The design and analysis of the FSCRP antenna model are carried out with the HFSS tool, and the antenna is tested using a vector network analyzer which is available in our laboratory. The FSCRP antenna prototype is presented in Fig. 5(a). The measurement setup for testing the prototype with signal gen-

TABLE 3. Simulated and measured results of FSCRP antenna.

		Operating Frequency (GHz)	Reflection Coefficient (dB)	Bandwidth (MHz)
Simulated	Free Space	2.46	−33.9	390 (2.38 GHz to 2.77 GHz)
	On Layers	2.46	−36.97	800 (2.04 GHz to 2.84 GHz)
Measured	Free Space	2.42	−27.05	160 (2.35 GHz to 2.51 GHz)
	On Layers	2.46	−32.31	610 (2 GHz to 2.61 GHz)

TABLE 4. Comparison of FSCRP antenna model with the existing models.

Ref. No.	Antenna Size (mm^3)	Substrate Material	Operating Freq. (GHz)	Impedance Bandwidth (GHz)	Application
[5]	20 × 18.8 × 0.762	Rogers R04350	2.43, 5.2	-	WLAN
[6]	26 × 26 × 4		2.45	2.40–2.48	On-body communication
[12]	24 × 22 × 0.07	Polyimide	2.41	2.01–2.82	ISM
[13]	32 × 40 × 0.07	Polyimide	2.45	2.27–2.76	WBAN
[14]	27 × 27 × 1.6	FR-4		4.25–12.5	WBAN application
[16]	70.4 × 76.14 × 3.11	Ro3003C (Semi-flex)	1.57, 2.435	(1.56–1.59) (2.434–2.451	GPS/WLAN
[Proposed]	26 × 22 × 0.07	Polyimide	2.46	(2.38–2.77)	ISM band

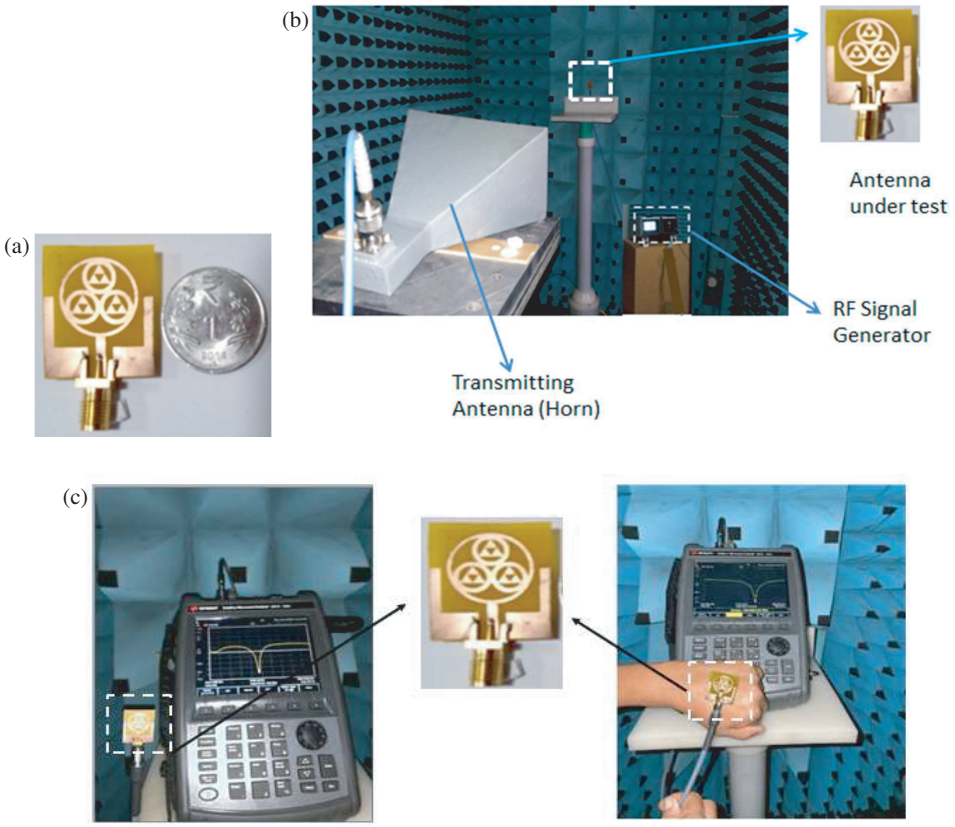

FIGURE 5. (a) Prototype of FSCRP antenna and measurement set-up for (b) Radiation pattern, (c) reflection coefficient in free space and on-human hand.

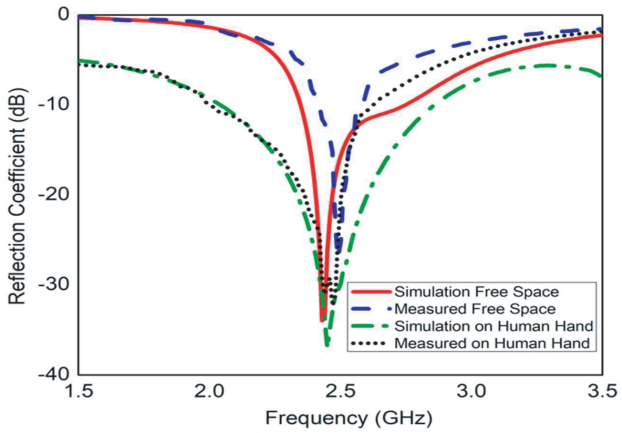

FIGURE 6. S_{11} of FSCRP antenna.

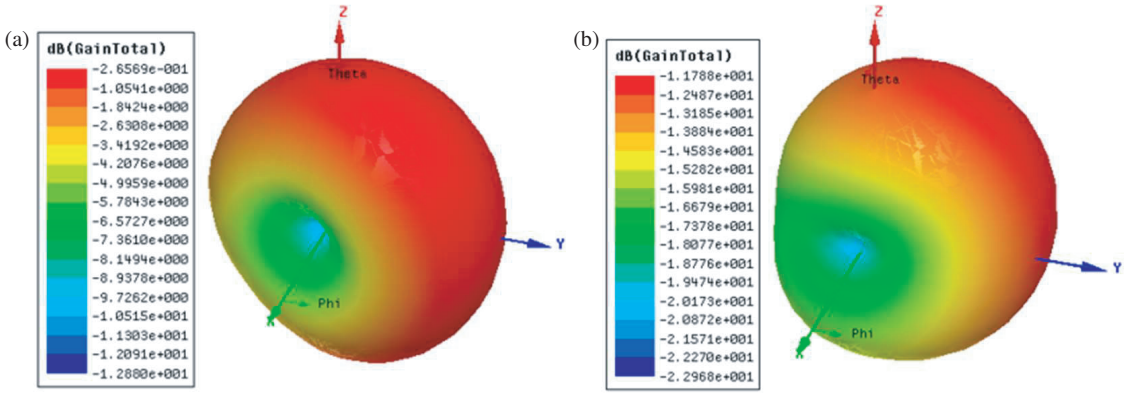

FIGURE 7. FSCRP antenna gain plot at 2.46 GHz frequency. (a) Free space. (b) On Human Han .

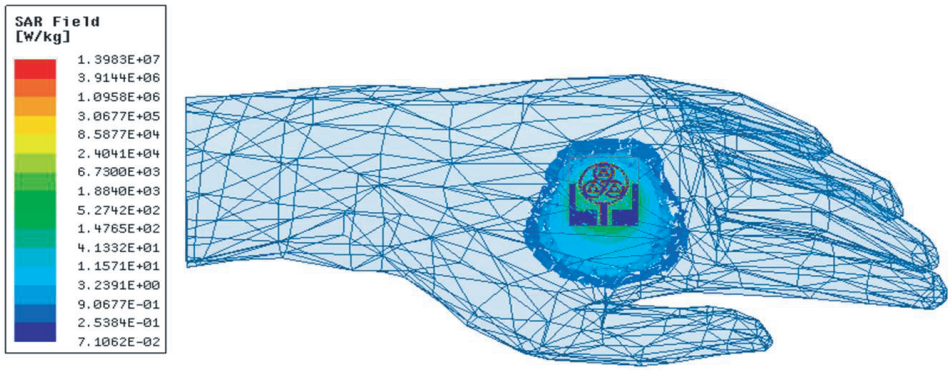

FIGURE 8. SAR of FSCRP antenna with layers at 2.46 GHz frequency.

erator and transmitting horn is shown in Fig. 5(b). The analysis has been carried out by placing the antenna in free space and on the three-layered tissue model of the human body. The measurement setup for the proposed FSCRP antenna model is shown in Fig. 5(c), concerning free space and on a human hand.

The S_{11} of the FSCRP model concerning simulated and measured is presented in Fig. 6. It is observed from the figure that the antenna operates at 2.46 GHz frequency on free space with bandwidth 390 MHz (2.38 GHz to 2.77 GHz) and reflection coefficient -33.7 dB, respectively. Similarly, on the three-layered tissue the antenna operates at 2.46 GHz with S_{11} of -36.97 dB and bandwidth of 800 MHz (2.04 GHz to 2.84 GHz). The comparison of simulated and measured results of the FSCRP antenna is tabulated in Table 3.

The 3D gain plot of the FSCRP antenna in free space and on the three-layered tissue is presented in Fig. 7. In free space the antenna produces a maximum gain of -0.265 dB and on the layered model with -11.78 dB, respectively.

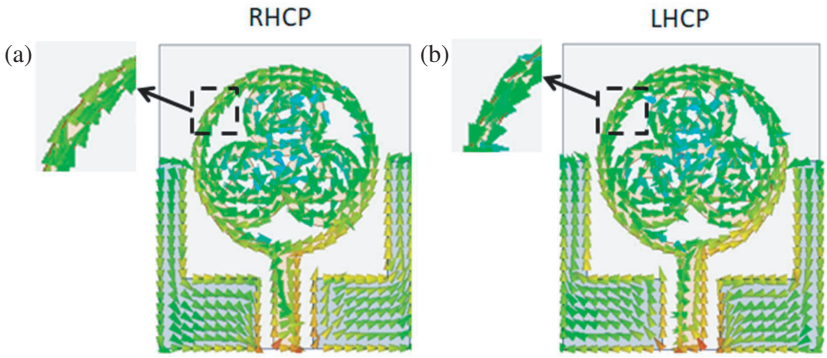

FIGURE 9. SCD of FSCRP antenna at 2.46 GHz frequency for ϕ. (a) 0°. (b) 90°.

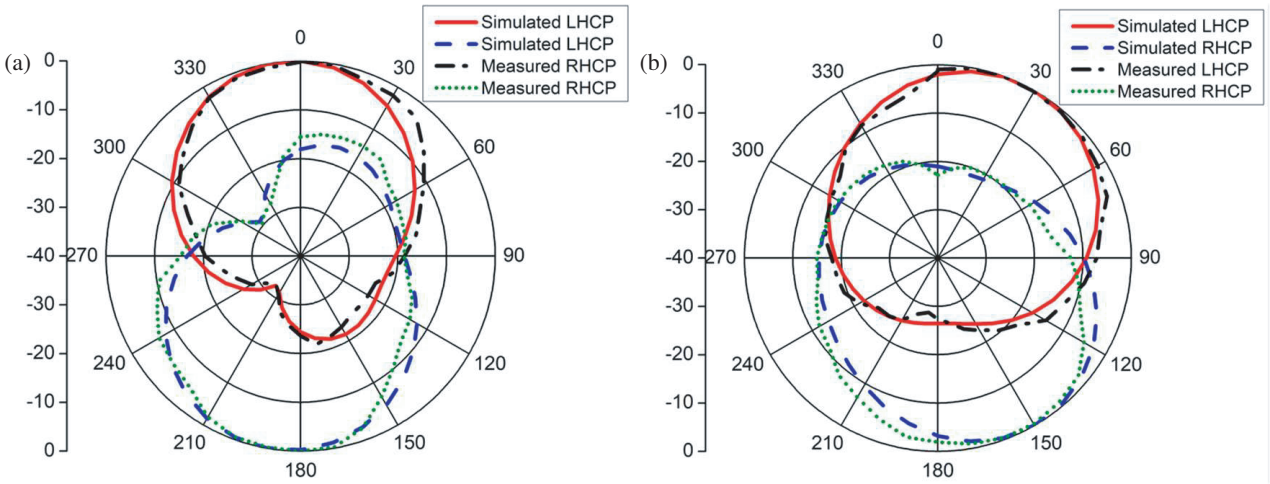

FIGURE 10. RP of FSCRP antenna at 2.46 GHz frequency. (a) XY-plane, and (b) YZ-plane.

The formula for calculating the SAR of the proposed antenna is given as

$$SAR = \frac{\sigma\,[E]^2}{\rho}\ \text{Watts/kg} \tag{1}$$

where σ is the conductivity of the tissue in S/m, E the electric field in V/m, and ρ the density of the tissue in g/cm^3.

The specific absorption rate (SAR) value corresponding to 1 g of tissue is less than 1.6 W/kg by IEEE.C95.1-1999 release in [11]. The SAR plot of the FSCRP antenna considered on the layer is shown in Fig. 8. A minimum value of 1.57 W/kg has been observed at 2.46 GHz frequency. Fig. 9 presents the surface current distribution (SCD) of the FSCRP antenna at 2.46 GHz frequency with respect to ϕ as 0° and 90°. Fig. 9(a) presents the SCD for $\phi = 0°$ where the antenna produces a right-hand circular polarization (RHCP), and Fig. 9(b) presents the SCD for $\phi = 90°$in which the antenna produces left-hand circular polarization, respectively.

The measured and simulated patterns of FSCRP antenna at 2.46 GHz frequency for XY and YZ-plane are shown in Fig. 10, concerning left hand circular polarization (LHCP) and right hand circular polarization (RHCP), respectively. From the plot, the patterns show an equal magnitude with a phase shift of 180° for both E and H-planes. The measured radiation patterns of FSCRP antenna is obtained in accordance to the testing environment as shown in Fig. 5(b). Fig. 11 shows the simulated and measured axial ratios of the FSCRP antenna. The simulated axial ratio of 0.5 dB (2.4–2.57 GHz) and measured value of 0.88 dB (2.4–2.5 GHz) are observed at 2.46 GHz frequency.

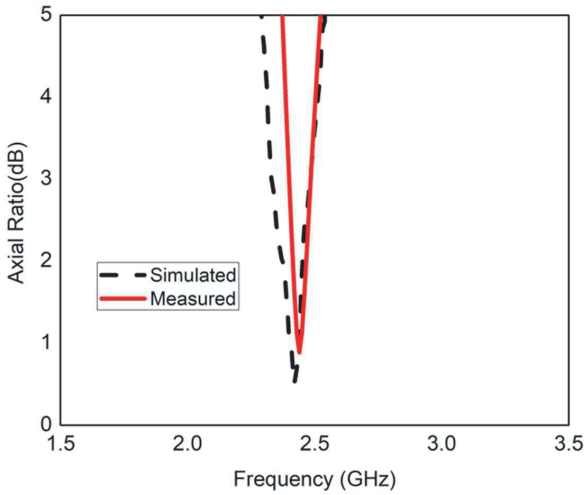

FIGURE 11. Axial ratio of FSCRP antenna.

The efficiency plot for the FSCRP antenna is shown in Fig. 12. A maximum efficiency of 75% is observed at 2.46 GHz frequency. The comparison of the proposed FSCRP antenna model to reference models is listed in Table 4.

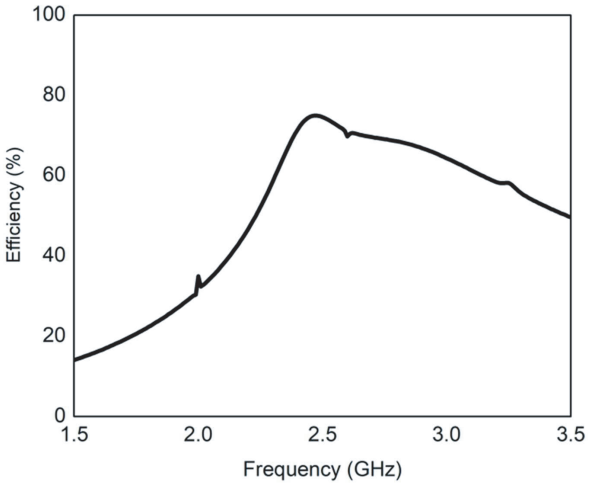

FIGURE 12. Efficiency plot of FSCRP antenna.

5. CONCLUSION

A novel design of a flexible fractal shape circular ring patch (FSCRP) antenna with CPW feed is presented for the ISM band with circular polarization in this paper. The FSCRP antenna functions from 2.42 GHz to 2.8 GHz in free space and from 2.08 GHz to 2.91 GHz under three layered human body structures. A SAR value of 1.57 W/kg is observed at 2.46 GHz operating frequency. The circular ring patch antenna helps to get circular polarization, and the axial ratio of the proposed antenna is observed in both simulation and measurement to be 0.5 dB and 0.88 dB at 2.46 GHz frequency. The proposed FSCRP antenna model is designed and used for biomedical applications at the ISM band.

ACKNOWLEDGEMENT

This work was supported by the Science and Engineering Research Board (SERB), Department of Science and Technology, New Delhi, India Grant No.'s: EEQ/2016/000754.

REFERENCES

[1] Kiourti, A., K. A. Psathas, and K. S. Nikita, "Implantable and ingestible medical devices with wireless telemetry functionalities: A review of current status and challenges," *Bioelectromagnetics*, Vol. 35, No. 1, 1–15, 2014.

[2] Raad, H. K., H. M. Al-Rizzo, A. Abbosh, and A. I. Hammoodi, "A compact dual band polyimide based antenna for wearable and flexible telemedicine devices," *Progress In Electromagnetics Research C*, Vol. 63, 153–161, 2016.

[3] Hall, P. S., Y. Hao, Y. I. Nechayev, A. Alomainy, C. C. Constantinou, C. Parini, M. R. Kamarudin, T. Z. Salim, D. T. M. Hee, R. Dubrovka, and e. al., "Antennas and propagation for on-body communication systems," *IEEE Antennas and Propagation Magazine*, Vol. 49, No. 3, 41–58, Jun. 2007.

[4] Kiourti, A. and K. S. Nikita, "A review of implantable patch antennas for biomedical telemetry: Challenges and solutions," *IEEE Antennas and Propagation Magazine*, Vol. 54, No. 3, 210–228, 2012.

[5] Salih, A. A. and M. S. Sharawi, "A dual-band highly miniaturized patch antenna," *IEEE Antennas and Wireless Propagation Letters*, Vol. 15, 1783–1786, 2016.

[6] Naik, K. K., P. A. V. Sri, and J. Srilakshmi, "Design of implantable monopole inset-feed c-shaped slot patch antenna for bio-medical applications," in *2017 Progress in Electromagnetics Research Symposium - Fall (PIERS - FALL)*, 2645–2649, Singapore, 2017.

[7] Poonkuzhali, R., Z. C. Alex, and T. N. Balakrishnan, "Miniaturized wearable fractal antenna for military applications at VHF band," *Progress In Electromagnetics Research C*, Vol. 62, 179–190, 2016.

[8] Çelenk, E. and N. T. Tokan, "All-textile on-body antenna for military applications," *IEEE Antennas and Wireless Propagation Letters*, Vol. 21, No. 5, 1065–1069, May 2022.

[9] Alrawashdeh, R. S., Y. Huang, M. Kod, and A. A. B. Sajak, "A broadband flexible implantable loop antenna with complementary split ring resonators," *IEEE Antennas and Wireless Propagation Letters*, Vol. 14, 1506–1509, 2015.

[10] Gani, I. and H. Yoo, "Multi-band antenna system for skin implant," *IEEE Microwave and Wireless Components Letters*, Vol. 26, No. 4, 294–296, 2016.

[11] Gabriel, S., R. W. Lau, and C. Gabriel, "The dielectric properties of biological tissues: III. Parametric models for the dielectric spectrum of tissues," *Physics in Medicine & Biology*, Vol. 41, No. 11, 2271, 1996.

[12] Ketavath, K. N., D. Gopi, and S. S. Rani, "In-vitro test of miniaturized CPW-fed implantable conformal patch antenna at ISM band for biomedical applications," *IEEE Access*, Vol. 7, 43 547–43 554, 2019.

[13] Yin, B., J. Gu, X. Feng, B. Wang, Y. Yu, and W. Ruan, "A low SAR value wearable antenna for wireless body area network based on AMC structure," *Progress In Electromagnetics Research C*, Vol. 95, 119–129, 2019.

[14] Kumar, V. and B. Gupta, "On-body measurements of SS-UWB patch antenna for WBAN applications," *AEU — International Journal of Electronics and Communications*, Vol. 70, No. 5, 668–675, 2016.

[15] Wong, K.-L., H.-J. Chang, C.-Y. Wang, and S.-Y. Wang, "Very-low-profile grounded coplanar waveguide-fed dual-band WLAN slot antenna for on-body antenna application," *IEEE Antennas and Wireless Propagation Letters*, Vol. 19, No. 1, 213–217, Jan. 2020.

[16] Yao, J., F. M. Tchafa, A. Jain, S. Tjuatja, and H. Huang, "Far-field interrogation of microstrip patch antenna for temperature sensing without electronics," *IEEE Sensors Journal*, Vol. 16, No. 19, 7053–7060, 2016.

[17] Sanders, J. W., J. Yao, and H. Huang, "Microstrip patch antenna temperature sensor," *IEEE Sensors Journal*, Vol. 15, No. 9, 5312–5319, 2015.

[18] Paracha, K. N., S. K. A. Rahim, P. J. Soh, M. R. Kamarudin, K.-G. Tan, Y. C. Lo, and M. T. Islam, "A low profile, dual-band, dual polarized antenna for indoor/outdoor wearable application," *IEEE Access*, Vol. 7, 33 277–33 288, 2019.

[19] Dash, S. K. K., T. Khan, and B. K. Kanaujia, "Circularly polarized dual facet spiral fed compact triangular dielectric resonator antenna for sensing applications," *IEEE Sensors Letters*, Vol. 2, No. 1, 1–4, Mar. 2018.

[20] Yang, Z.-J., S.-Q. Xiao, L. Zhu, B.-Z. Wang, and H.-L. Tu, "A circularly polarized implantable antenna for 2.4-GHz ISM band biomedical applications," *IEEE Antennas and Wireless Propagation Letters*, Vol. 16, 2554–2557, 2017.

[21] Xu, L.-J., Y.-X. Guo, and W. Wu, "Miniaturized circularly polarized loop antenna for biomedical applications," *IEEE Transactions on Antennas and Propagation*, Vol. 63, No. 3, 922–930, 2015.

[22] Liu, C., Y. Zhang, and X. Liu, "Circularly polarized implantable antenna for 915 MHz ISM-band far-field wireless power transmission," *IEEE Antennas and Wireless Propagation Letters*, Vol. 17, No. 3, 373–376, 2018.

[23] Zhang, K., C. Liu, X. Liu, H. Guo, and X. Yang, "Miniaturized circularly polarized implantable antenna for ISM-band biomedical devices," *International Journal of Antennas and Propagation*, Vol. 2017, No. 1, 9750257, 2017.

[24] Liu, C., Y.-X. Guo, R. Jegadeesan, and S. Xiao, "In vivo testing of circularly polarized implantable antennas in rats," *IEEE Antennas and Wireless Propagation Letters*, Vol. 14, 783–786, 2014.

[25] Das, S. and D. Mitra, "Design of a compact circular polarized implantable ring slot antenna for biomedical applications," *Electromagnetics*, Vol. 40, No. 2, 83–92, 2020.

[26] Xu, L.-J., Y. Bo, W.-J. Lu, L. Zhu, and C.-F. Guo, "Circularly polarized annular ring antenna with wide axial-ratio bandwidth for biomedical applications," *IEEE Access*, Vol. 7, 59 999–60 009, 2019.

[27] Ramzan, M., A. Khaleghi, X. Fang, Q. Wang, N. Neumann, and D. Plettemeier, "An ultra-miniaturized high efficiency implanted spiral antenna for leadless cardiac pacemakers," *IEEE Transactions on Biomedical Circuits and Systems*, Vol. 17, No. 3, 621–632, Jun. 2023.

[28] Wang, M., H. Liu, P. Zhang, X. Zhang, H. Yang, G. Zhou, and L. Li, "Broadband implantable antenna for wireless power transfer in cardiac pacemaker applications," *IEEE Journal of Electromagnetics, RF and Microwaves in Medicine and Biology*, Vol. 5, No. 1, 2–8, Mar. 2021.

[29] Ganeshwaran, N., J. K. Jeyaprakash, M. G. N. Alsath, and V. Sathyanarayanan, "Design of a dual-band circular implantable antenna for biomedical applications," *IEEE Antennas and Wireless Propagation Letters*, Vol. 19, No. 1, 119–123, Jan. 2020.

[30] Naik, K. K., S. C. S. Teja, B. V. Sailaja, and P. A. Sri, "Design of flexible parasitic element patch antenna for biomedical application," *Progress In Electromagnetics Research M*, Vol. 94, 143–153, 2020.

[31] Kumar, R. and S. Singh, "Cpw fed conformal PIFA design for implantable iomt devices with wideband performance," *IEEE Sensors Journal*, Vol. 24, No. 1, 231–237, Jan. 2024.